

General Disclaimer

One or more of the Following Statements may affect this Document

- This document has been reproduced from the best copy furnished by the organizational source. It is being released in the interest of making available as much information as possible.
- This document may contain data, which exceeds the sheet parameters. It was furnished in this condition by the organizational source and is the best copy available.
- This document may contain tone-on-tone or color graphs, charts and/or pictures, which have been reproduced in black and white.
- This document is paginated as submitted by the original source.
- Portions of this document are not fully legible due to the historical nature of some of the material. However, it is the best reproduction available from the original submission.

**NASA TECHNICAL
MEMORANDUM**

NASA TM X-71858

NASA TM X-71858

(NASA-TM-X-71858) DESIGN AND PERFORMANCE
VERIFICATION OF ADVANCED MULTISTAGE
DEPRESSED COLLECTORS (NASA) 12 p HC \$3.50
CSCI 09A

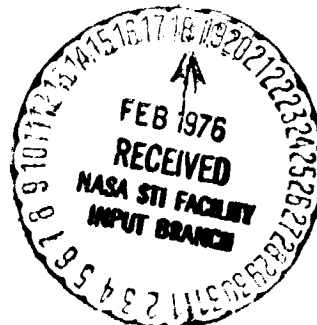
N76-18346

Unclas
G3/33 13595

**DESIGN AND PERFORMANCE VERIFICATION OF ADVANCED
MULTISTAGE DEPRESSED COLLECTORS**

by H. Kosmahl and P. Ramins
Lewis Research Center
Cleveland, Ohio 44135

TECHNICAL PAPER presented
International Electron Devices Meeting sponsored by
the Institute of Electrical and Electronics Engineers
Washington, D.C., December 1-3, 1975



ABSTRACT

Design and performance of a small size, 4-stage depressed collector are discussed. The collector and a spent beam refocusing section preceding it are intended for efficiency enhancement of octave bandwidth, high cw power traveling wave tubes for use in ECM. The work reported herein is a joint effort between the USAF and NASA Lewis Research Center.

DESIGN AND PERFORMANCE VERIFICATION OF ADVANCED MULTISTAGE DEPRESSED COLLECTORS

H. Kosmahl and P. Ramins
National Aeronautics and Space Administration
Lewis Research Center
Cleveland, Ohio

SUMMARY

In a joint USAF-NASA Program, Lewis Research Center is carrying out an efficiency improvement program on TWTs for use in ECMs by applying multistage depressed collector (MDC) and spent beam refocusing techniques developed at Lewis. In the analytic part of the effort, 3-D electron trajectories are used throughout the 10-18 percent electronically efficient TWT with a 4.8-9.6 GHz bandwidth and 400-600 W CW power output. Trajectory computation continues through the spent beam refocuser and the depressed collector. Collector efficiency, collector losses and overall efficiency are identified and computed. On the experimental side, tube performance is evaluated first without the MDC, then the spent beam is analyzed for symmetry, circularity and the velocity spread which permits determination of the size of the apertures. Finally, the MDC is attached and its performance optimized and evaluated. 3-D theory, for ideal tubes, predicts a MDC-efficiency, at mid-band, of 84 percent for a 4 stage MDC with symmetric, circular and optimally refocused beams.

Experimental results to date have yielded an MDC efficiency of 72 percent at mid-band.

INTRODUCTION

The proliferation of the electronic warfare threat in frequency spectrum and power level introduces a requirement for much more efficient ECM-systems than have been acceptable in the past. Since the internal electronic efficiency cannot be improved much in broad band ECM tubes, the only effective means is the application of advanced MDCs in conjunction with spent beam refocusing methods to achieve high overall efficiency. Although some simple depressed collectors are being used in ECM-TWTs, the improvement in efficiency that can be achieved with them is too small to be acceptable to modern high power ECM systems.

In a joint effort with the USAF, NASA-Lewis is adapting the efficiency enhancement schemes developed at Lewis to ECM-TWTs delivered by the USAF. These methods were successfully demonstrated in the CTS-Project in which an overall efficiency of 56 percent achieved at 12GHz in a communications TWT by a MDC working at 81 percent efficiency level.

The requirements of the AF-System call, however, for a much smaller collector size and fewer electrodes than with the CTS-TWT. Also, beam space charge and perveance are much higher than in NASA communication tubes. On the other hand, electronic efficiencies are only about half as large (10-18 percent) as the CTS tube. Thus, methods developed previously must be adapted to a completely new set of requirements and parameters. The results of the initial phase of analytic and experimental studies are discussed in the following sections.

DESIGN CRITERIA FOR THE MDC

It can be shown (ref. 1) that in all axisymmetric, magnetic field free MDCs, highest efficiencies are obtained only when the collector size and lengths of all trajectories are large compared to beam size (point source). This is so because an electrostatic MDC must convert a small part of the injection energy into radial deflection to accomplish sorting into energy classes (sorting efficiency). Figure 1 shows a sample of actually computed electron trajectories plus one test electron. The latter was injected with a (representative) angle of $+3^\circ$ and a total kinetic energy of $+0.5 V_0$. At the apex it approaches an equipotential line at $-0.485 V_0$; thus, it could be, in principle, collected with 97 percent efficiency. If more deflection is applied, the beam spreads farther away from axis, electron penetration is less deep and the sorting efficiency lower. It turns out that the best aperture size is the smallest opening through which almost all trajectories can penetrate. Figure 2 shows extremely small negative angles, and Figure 3, large positive angles as the other side of extreme entrance conditions. Thus, the aperture size is determined by the largest radial velocity components in the beam which, in turn, depend partially on the quality of refocusing. It has been shown (ref. 3) that the RMS value of the radial velocity spread can be reduced in this application by a factor of 2 to 3 when an optimum expansion in the refocuser is applied. Simultaneously, the space charge is diluted such as to become unimportant in the collector region.

Figure 4 shows schematically the principle of magnetic refocusing, originated and developed at LeRC (ref. 2). As the beam expands in a decaying magnetic field (it could be permanent magnet field with a reversal) transverse velocities are transformed in axial motion. Note that this arrangement is very different conceptually from an application of a simple magnetic lens to the end of the tube. Such an additional magnetic lens squeezes the spreading spent beam and permits smaller entrance angle conditions into the collector. It does, however, increase the radial velocity spread later on which leads to larger losses in collector efficiency (than achievable with optimum refocusing).

ANALYSIS OF COLLECTOR INEFFICIENCY

Direct 3-D computation of actual electron trajectories for ideal conditions permits a determination of collector inefficiency as well as sources thereof. Figure 5 identifies six sources. The first four are due to losses caused by a

symmetric, circular and optimally refocused beam. When the beam is asymmetric, and/or noncircular, the optimum design must be compromised by creating larger apertures and changing the location of electrodes, resulting in smaller than optimum collector efficiency, the loss depending on the degree of asymmetry and noncircularity. In "Non-ideal Tubes" all effects are summed up which cause a deviation of computed trajectories from the actual ones, e. g., incorrect beam radius, cocked guns, internal reflections, distortions in the potential due to supporting rods, deviations in the ppm-stock, etc. Obviously an estimate or calculation of these sources is possible only when quantitative data are available. We feel, however, that 5 percent or more percentage points loss in η_{col} is certainly possible depending on the degree of deviation from ideal conditions.

EXPERIMENTAL

Experimental evaluations include: RF power, TWT body power, and collector power measurements on the tube with an underpressed collector; calorimetric and electric spent beam tests; and tests with MDCs attached. Currents, voltages and thermal power dissipation are determined on each MDC-electrode in vacuum better than 2×10^{-9} torr. Optimization of MDC-performance is accomplished by: changing the refocusing field, the depth of the spike and the potentials of the electrodes. Changes in aperture sizes and electrode distribution are made by closing a special Ultra High Vacuum Valve, removing the tested MDC, and replacing it with a modified version. Figure 6 shows a view of the experimental set-up.

Figure 7 shows the apparatus for analyzing the spent beam. A segmented collector-calorimeter is mounted 12 inches from the exhaust of the tube. Both, current and power in each segment can be determined as well as the symmetry and circularity of the beam. A photograph of the beam image is shown in Fig. 8. Observe some asymmetry and noncircularity. Approximately 10 percent of power is outside the injection angle of 7° , while theory predicts all power to be within 5.9° . This discrepancy can be in part explained by the need to focus the beam through an $1/3$ in. long field free tunnel which houses the UHV valve. In order to pass the beam through this field free length, it has to be prematurely over-focused and expands too soon at the entry into the collector. The UHV valve and its tunnel housing would not, of course, be necessary in actual tubes.

Figure 9 shows the setup with MDC, spike motion and refocusing. Thermal and electric power measurements, accurate to 1-2 percent are made for each collector electrode. Measurements were made with an MEC high perveance tube. Figure 10 shows RF power out and RF helix losses versus frequency. The RF losses are much higher than cold helix measurements predict and the circuit efficiency is at some frequencies as low as $\eta_{CT} \approx 0.6$.

With the asymmetric beam and too wide beam the collector efficiency was measured and is shown in Figure 11. The computed number was 84 percent for a max injection angle of 5.9° and would be certainly smaller for larger injection angles.

In addition to collector efficiency, Figure 11 indicates the voltages, the currents and the power dissipated on each collector electrode. The voltages have been selected to optimize the collector efficiency at midband (highest power output). Several important conclusions can be drawn: first, the current to the grounded plate is 32 mA and not zero. Part of this loss is due to asymmetry. Secondary suppressing coatings offer certainly some remedy, but were not tried.

Secondly, the average KV per electron dissipated on each electrode can be calculated by dividing P/I_c . This KeV number should be approximately equal in the ideal case to one half of the voltage difference between the adjacent plates. It is, however, larger. This loss can be most convincingly explained by postulating that each electrode is struck by some electrons on its low side. These electrons give up all kinetic energy as heat, yield at least one secondary each which moves down to the next plate with an energy consumption of $e \cdot \Delta V$. The performance presented here is preliminary and the optimization work is being continued.

What causes the 12 percent point difference between computed and measured efficiencies ?

First, the collector would like to see a more expanded and better collimated beam than the present $1/4$ in. tunnel housing the UHV valve permits. Secondly, secondaries escape through open spaces to ground potential. Thirdly, the potentials between plates are distorted by the lateral smallness of the electrodes (2 in. diameter). And finally there is still some asymmetry. Corrections of these problems should bring η_{col} to 80 percent or more. With a dc beam, the collector efficiency is already now in excess of 90 percent, which indicates excellent sorting ability of the collector. The overall efficiency at midband is now 30 percent. With $\eta_{CT} = 0.9$ instead of 0.7 and $\eta_{col} \approx 0.8$ instead of 0.72, η_{ov} would become 48 percent.

CONCLUDING REMARKS

Experimental results obtained from three iterations of a small size (3 in. x 2 in.) MDC which was operated as an efficiency boosting device in conjunction with a broad band, high power ECM-TWT indicate a discrepancy between computed (84 percent) and measured (72 percent) results in collector efficiency at maximum power output at midband. The causes of this discrepancy are only partially understood because a closer agreement was expected with the 3-D calculations. The unknown factors include all deviations present in practical tubes

and collectors from ideal parameters. Further diagnostics are planned and expected to narrow the gap between theory and experiment. The TWT being evaluated exhibited much higher circuit losses than was generally assumed in industry and the DOD, that is a circuit efficiency of 60 percent to 70 percent instead of 90 percent. With a collector efficiency, η_{col} , improvement to 80 percent and circuit efficiency η_{CT} at the present level overall tube efficiencies would be limited to about 35 percent. Intensive work on circuit losses is required to fully realize the potential improvement in overall efficiency.

REFERENCES

- (1) H. Kosmahl, "A Novel, Axisymmetries, Electrostatic Collector," NASA TN D-6093, February 1971.
- (2) H. Kosmahl, D. McNary, and O. Sauseng, "High Efficiency, 200-Watt 12-Gigahertz TWT," NASA TN D-7709, June 1974.
- H. Kosmahl, O. Sauseng, and B. D. McNary, "A 240-Watt 12-GHz Space Communication TWT with 56 % Overall and 81 % Collector Efficiency," IEEE TRANS. Education, Vol. ED-20, December 1973.
- (3) N. Stankiewicz, "Evaluation of Magnetic Refocusing in Linear Beam Tubes," NASA TN D-7660, June 1974.

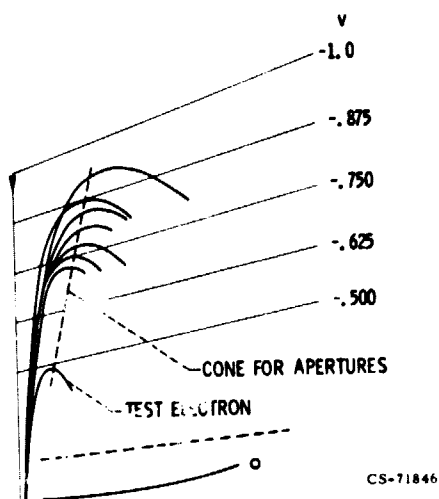


Figure 1. - Actual electron trajectories for average injection angles.

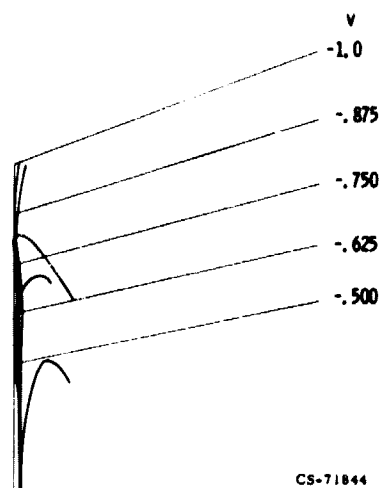


Figure 2. - Actual electron trajectories for small negative injection angles.

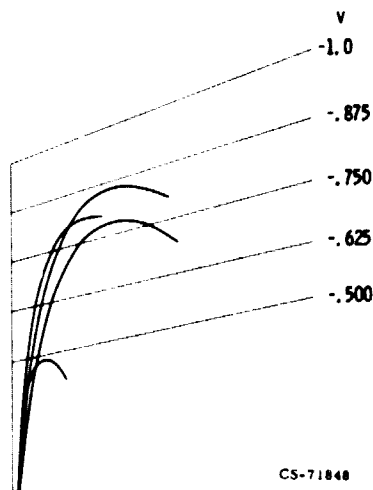


Figure 3. - Actual electron trajectories for large positive injector angles.

ORIGINAL PAGE IS
OF POOR QUALITY

PRECEDING PAGE BLANK NOT FILMED

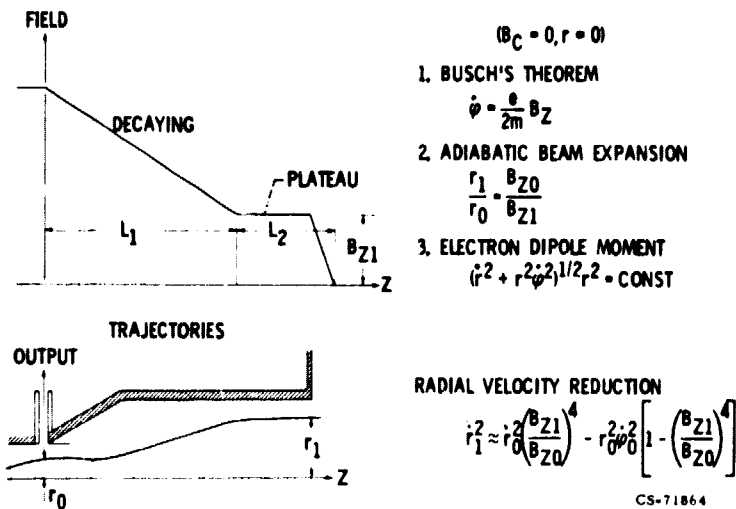


Figure 4. - Schematic of the spent beam refocusing system.

- | | |
|---|-----|
| 1. FINITE NO. OF ELECTRODES (5) COMPARED WITH INFINITE NO. | 5 |
| 2. RADIAL VELOCITY SORTING | 3 |
| 3. VERY LARGE ANGLES ($> 6^\circ$) & VERY SMALL ANGLES ($< 0.25^\circ$) | 4 |
| 4. SECONDARIES ON CONE & ELSEWHERE | 1-2 |
| 5. ASYMMETRY & NONCIRCULARITY OF THE BEAM | |
| 6. NONIDEAL TUBES | |

CS-71849

Figure 5. - Analysis of collector inefficiency with good refocusing.

ORIGINAL PAGE IS
OF POOR QUALITY

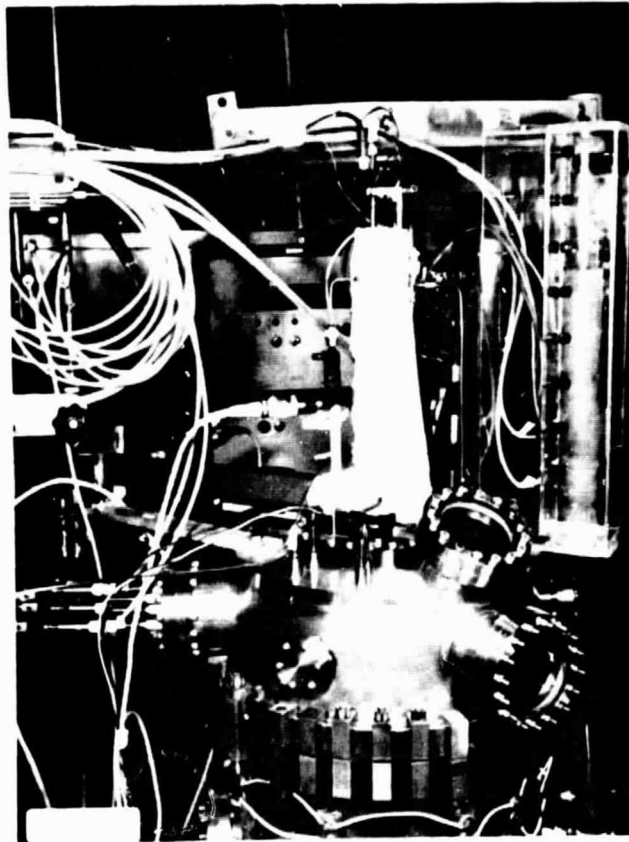
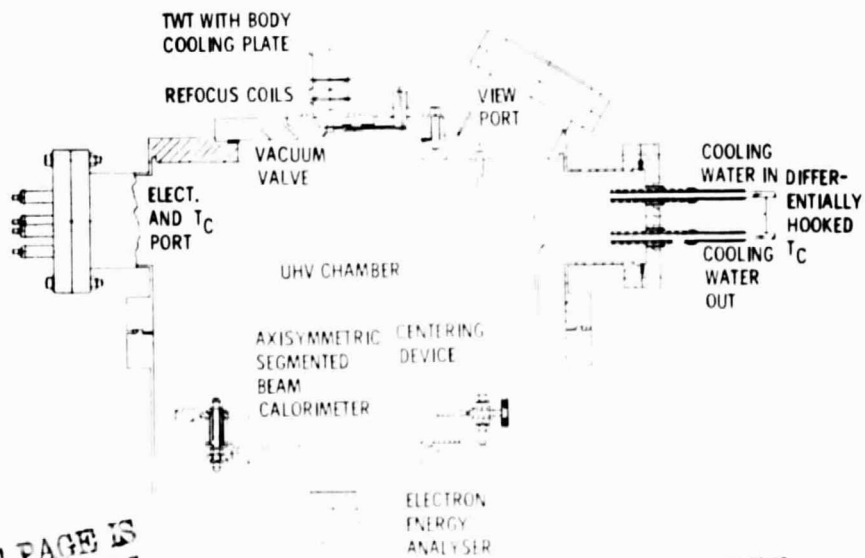


Figure 6. - Vacuum tank with TWT mounted on top.



TWT BEAM TEST SET-UP

Figure 7. - Schematic of the spent beam measuring set-up.

ORIGINAL PAGE IS
OF POOR QUALITY

OS-75417

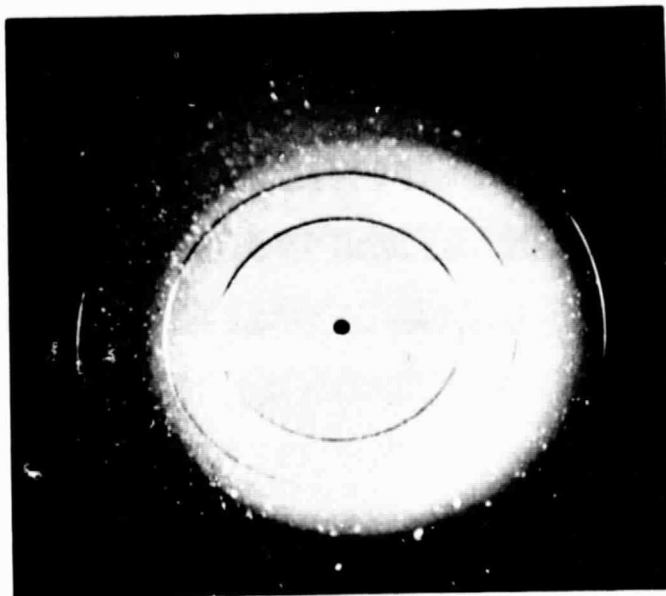


Figure 8. - Spent beam cross-section after refocusing.

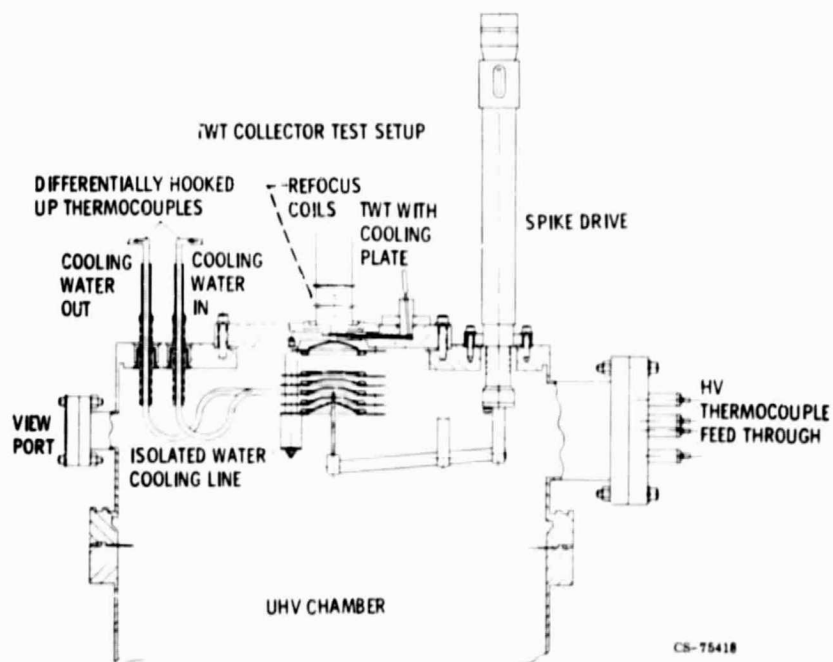


Figure 9. - Schematic of the MDC measuring system.

ORIGINAL PAGE IS
OF POOR QUALITY

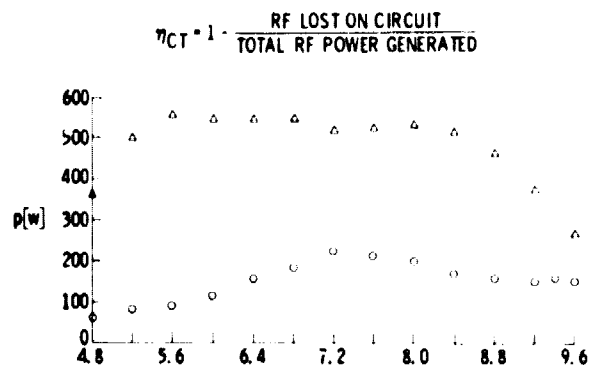


Figure 10. - Output power and circuit loss power of the TWT versus frequency.

CS-75416

SATURATED OUTPUT 7.2 GHz

I_C mA	P_{id} W	V_{col} kV
32	188	0
50	64	4.53
131	209	4.70
75	66	7.45
133	277	8.24
-7	13	9.50

MECTWT 300-600 W
 $V_0 = 9.45$ kV; $I_0 = 436$ mA
 $I_B = 18$ mA

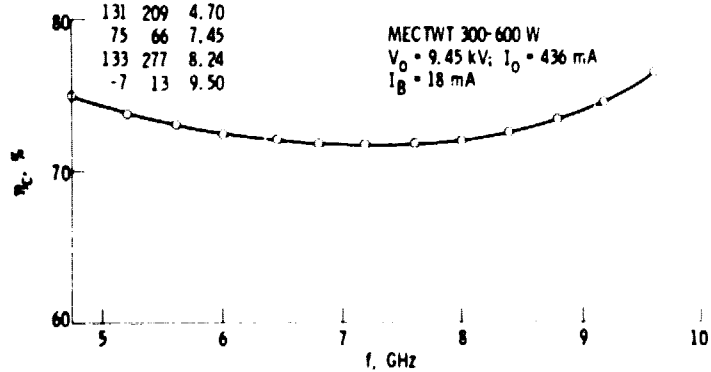


Figure 11. - Collector efficiency versus frequency.